Effects of Density on the Intramolecular Hydrogen Bonding, Tail−Tail Cyclization, and Mean-Free Tail-to-Tail Distances of Pyrene End-Labeled Poly(dimethylsiloxane) Oligomers Dissolved in Supercritical CO_2

Maureen A. Kane, Siddharth Pandey,† Gary A. Baker, Sherryl A. Perez, Eric J. Bukowski, David C. Hoth, and Frank V. Bright*

Department of Chemistry, Natural Sciences Complex, University at Buffalo, The State University of New York, Buffalo, New York 14260-3000

Received May 14, 2001; Revised Manuscript Received July 13, 2001

ABSTRACT: We report on the steady-state and time-resolved fluorescence from poly(dimethylsiloxane) oligomers that have been end-labeled with pyrene (Py-PDMS-Py) when it is dissolved in supercritical CO_2 between a reduced density ($\rho_r = \rho_{experiment}/\rho_{critical}$) of 0.7 and 2.3. In a good solvent like liquid toluene, the Py-PDMS-Py excimer formation follows a classic Birks scheme with a homogeneous ground state. In supercritical CO_2 there are at least two forms of Py-PDMS-Py (constrained and unconstrained) in the ground state prior to photoexcitation. The constrained species arises from intramolecular hydrogen bonding between the opposing peptide segments within the Py-PDMS-Py terminal region that were introduced during labeling. This ground-state, hydrogen-bonded species precludes normal excimer formation. The unconstrained species leads to classic excimer formation. The constrained/intramolecularly hydrogen-bonded species dominates at lower CO_2 densities (86 ± 2% contribution at $\rho_r = 1.40$); however, its dominance wanes as the CO_2 density increases (14 ± 2% contribution at $\rho_r = 1.95$). There is also evidence that the known changes in the PDMS chain correlation length with CO_2 density influence the Py-PDMS-Py tail−tail dynamics. The mean-free distance between the Py-PDMS-Py termini also depends on the CO_2 density. At low CO_2 densities, the Py residues on the unconstrained Py-PDMS-Py molecules are closer together on average than they are at higher CO_2 densities. However, in supercritical CO_2, the unconstrained Py-PDMS-Py termini are never as far apart, on average, as they are when Py-PDMS-Py is dissolved in a good solvent like liquid toluene. This result is consistent with previous continuous space Monte Carlo simulations. Our results are also consistent with the presence of upper and lower critical solution pressures/densities for dilute PDMS dissolved in supercritical CO_2.

Introduction

In liquids polymer conformation, dynamics, and reactivity depend on whether the polymer is dissolved in a "good", "Θ", or "poor" solvent.[1−3] Thus, one can control polymer behavior, growth, and/or reactivity by switching from one solvent to another. Although solvent switching offers a powerful strategy for effecting control over a polymer system, many liquids (e.g., CH_2Cl_2) are not particularly environmentally responsible.[4]

Supercritical fluids exhibit liquidlike densities and gaslike mass transport properties, some are considered environmentally responsible, and one can control the physicochemical properties (e.g., density, dielectric constant, refractive index, compressibility) of a supercritical fluid by adjusting the system pressure and/or temperature.[5−12] Thus, supercritical fluids are often described as being continuously tunable solvents. Supercritical CO_2 ($scCO_2$) is an especially attractive fluid because one can easily access its critical temperature ($T_c = 31.1$ °C) and pressure ($P_c = 73.8$ bar), it is relatively inexpensive, it is nonflammable and nontoxic, it can be easily separated from many solutes by using a decompression step, it can be recycled and reused, and it is an environmentally responsible solvent.[5−12]

Over the past several years, DeSimone[13] and his research team have shown that one can carry out a wide variety of polymerization reactions by using $scCO_2$ as the reaction solvent. However, there is a dearth of molecular-level information[14−16] regarding the actual conformation and dynamics of dilute polymer solutions dissolved in $scCO_2$ and cosolvent-modified CO_2 over a wide density range. There is also a related body of literature on the use of CO_2-philic polymers/oligomers (i.e., fluoropolymers and polysiloxane) to solubilize a wide variety of reagents (e.g., metal chelators, catalysts), as stabilizers for dispersion polymerization, and as a means to prepare graft copolymers that can form micelles in $scCO_2$.[17,18] Here again, one finds little direct information on the precise behavior of the polymer/oligomer tail groups and other reactive subunits within the polymer/oligomer as a function of CO_2 density, added cosolvents, and polymer/oligomer chain length.

The behavior of tail segments within flexible molecules is of particular importance because tails represent the sites at which chain growth occurs during polymerization, tails can wrap around a tethered reactive site to block it from access, and tails can react with one another to form cyclic structures. One of the more attractive ways to investigate the behavior of flexible molecule termini is to site selectively label these "tails" with an excimer forming fluorophore like pyrene.[19−21] In this way one can address issues ranging from tail−tail cyclization/unfolding dynamics to inter- and intramolecular associations of chain termini/tails them-

† Current address: Department of Chemistry, New Mexico Institute of Technology, Socorro, NM 87801.

* To whom all correspondence should be directed. (716) 645-6800 ext 2162 (voice); (716) 645-6963 (Fax); chefvb@acsu.buffalo.edu (e-mail).

10.1021/ma010837u CCC: $20.00
Published on Web 08/17/2001

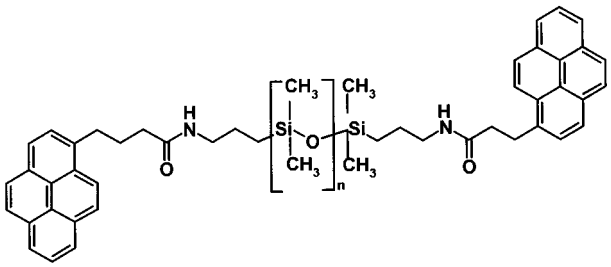

Figure 1. Chemical structure of pyrene end-labeled PDMS (Py-PDMS-Py).

Scheme 1

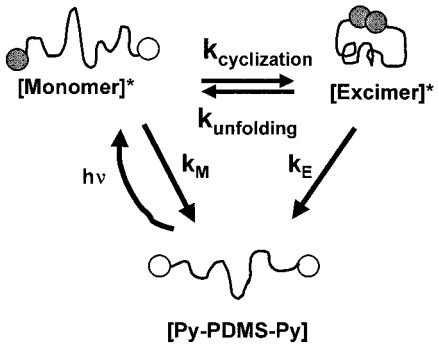

selves. Previous work has shown that the excimer emission depends on chain length and chain structure between the termini, the actual fluorophore chemistry one places at the chain termini, the exact labeling site on the fluorophore and the chain, the tether length and its chemistry, and the solvent quality/composition, temperature, and pressure.[19−21]

Our aim with this paper is to determine how the behavior and conformation of a simple polymer/oligomer chain, dissolved at low concentration (<10 μM) in $scCO_2$, are influenced by CO_2 density and the addition of a cosolvent. Toward these ends, we report on the behavior of poly(dimethylsiloxane) (PDMS) that has been selectively end-labeled with the fluorophore pyrene (Py-PDMS-Py, Figure 1)[16] when it is dissolved in $scCO_2$ or a binary mixture of CO_2 and 1 mol % MeOH.

Theory Section

Given the well-known limitations associated with the characterization of excimer emission from end-labeled polymers,[19−21] we can explore the possible models for an end-labeled polymer. In the most simple scenario, excimer emission from an end-labeled polymer can be described by using a variation of the classic Birks model (Scheme 1).[22,23] In this model k_M, k_E, $k_{cyclization}$, and $k_{unfolding}$ represent the unimolecular rates of monomer and excimer decay, tail cyclization, and chain/tail unfolding, respectively. Following electronic excitation by a short pulse of electromagnetic radiation, Scheme 1 predicts that the monomer time-resolved fluorescence intensity ($I_M(t)$) will decay as the *sum* of two exponentials, the excimer time-resolved emission intensity ($I_E(t)$) will decay as the *difference* of two exponentials

$$I_M(t) = a_1 \exp(-\lambda_1 t) + a_2 \exp(-\lambda_2 t) \quad (1)$$

$$I_E(t) = a_3 \exp(-\lambda_3 t) + a_4 \exp(-\lambda_3 t) \quad (2)$$

and certain decay constants (λ_i) must be identical (i.e., $\lambda_1 = \lambda_3$ and $\lambda_2 = \lambda_4$). If Scheme 1 describes the system

Scheme 2

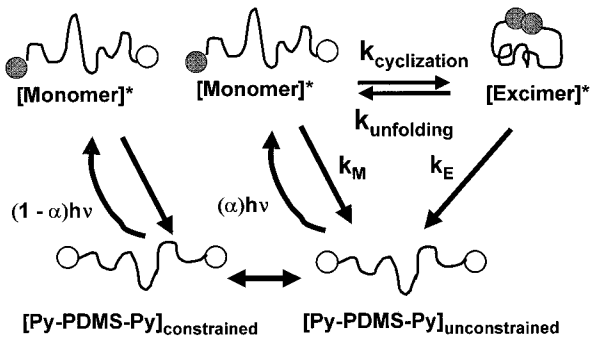

photophysics, one can recover all the kinetic terms from the following relationships:

$$2\lambda_{1 \text{ or } 3} = (A_x + A_y) - [(A_x - A_y)^2 + 4k_{cyclization}\, k_{unfolding}]^{1/2} \quad (3a)$$

$$2\lambda_{2 \text{ or } 4} = (A_x + A_y) + [(A_x - A_y)^2 + 4k_{cyclization}\, k_{unfolding}]^{1/2} \quad (3b)$$

where

$$A_x = k_M + k_{cyclization} \qquad A_y = k_E + k_{unfolding} \quad (4)$$

and

$$a_2/a_1 = (A_x - \lambda_1)/(\lambda_2 - A_x) \quad (5a)$$

$$a_4/a_3 = -1 \quad (5b)$$

if one knows k_M. In the current work we use the 1-ethylpyrene excited-state fluorescence lifetime τ_M as a measure of k_M ($k_M = 1/\tau_M$).

In some cases Scheme 1 (with it constraints) fails to describe the experimental time-resolved intensity decay data.[19−21] Under these circumstances, one must modify the basic Birks model to account for the presence of, for example, ground-state species that are preformed into an "excimer-like species" prior to optical excitation, a population of species that cannot cyclize to form an excimer, and/or populations of subspecies that can simultaneously form/deform an excimer along multiple pathways.[19−21] Scheme 2 is an example of a more complex model where there are two ground-state species: (1) an *unconstrained* species that can cyclize to form an excimer during the pyrene excited-state lifetime as in Scheme 1 and (2) a *constrained* species that cannot cyclize to form an excimer. The α term in Scheme 2 represents that fraction of the excitation beam that is absorbed by the unconstrained ground-state species.[24] If Scheme 2 operates, eqs 1−4 remain valid;[25] but one must modify eq 5 to account for the fraction of incident excitation energy, α, that is absorbed by the unconstrained ground-state species:

$$a_2/a_1 = [\alpha(A_x - \lambda_1) - (1 - \alpha)k_{folding}]/[\alpha(\lambda_2 - A_x) + (1 - \alpha)k_{unfolding} \quad (6a)$$

$$a_3/a_4 = [(1 - \alpha)(A_y - \lambda_1) - \alpha k_{cyclization}]/[(1 - \alpha)(\lambda_2 - A_y) + \alpha k_{cyclization}] \quad (6b)$$

Although numerous methods exist for recovering the kinetic terms from $I_M(t)$ and $I_E(t)$, we have opted to use a global analysis strategy.[26] In this approach, the

monomer and excimer decay profiles are simultaneously tested against a particular model (e.g., Schemes 1 or 2) such that a self-consistent set of kinetic terms are fit for and recovered. Global analysis also provides a more rigorous set of fitting criteria, it yields all the kinetic terms directly, and the accuracy of the recovered kinetic terms is improved significantly because multiple data sets are being fit to and modeled simultaneously.[26]

Experimental Section

Chemicals and Reagents. Aminopropyldimethyl-terminated poly(dimethylsiloxane) (NH_2-PDMS-NH_2) of 2500 g/mol average molecular weight (M_n) was purchased from United Chemical Technologies. 1-Pyrenebutanoic acid succinimidyl ester and 1-ethylpyrene were purchased from Molecular Probes, Inc. Anhydrous toluene (HPLC grade, 99.8+%) was a product of Sigma-Aldrich. MeOH (HPLC grade, 99.9%) was from Aldrich. CO_2 (SFC grade) was from Scott Specialty Gases. All chemicals and reagents were used as received.

Synthesis and Characterization of Py-PDMS-Py.[16] NH_2-PDMS-NH_2 was reacted in anhydrous toluene with a 10-fold molar excess of 1-pyrenebutanoic acid succinimidyl ester for 24 h with stirring in the dark under a N_2 atmosphere. The product was isolated by gel permeation chromatography, and its structure was confirmed by matrix-assisted laser desorption/ionization time-of-flight mass spectrometry (MALDI-TOF MS). Only the doubly labeled Py-PDMS-Py is present in our samples following purification.

Sample Preparation for Fluorescence Studies. All Py-PDMS-Py samples are loaded into the high-pressure cells by adding a small aliquot of Py-PDMS-Py dissolved in toluene, and the solvent is removed by using a gentle stream of Ar gas. Before pressurization, the high-pressure cells are flushed with CO_2 (~200 psi) for approximately 10−15 min to remove any residual O_2 and/or toluene. Experiments are typically carried out on samples that are between 1 and 5 μM in terms of the pyrene fluorophore.

Instrumentation. Steady-state excitation and emission experiments were performed by using an SLM-AMINCO model 48000 MHF fluorometer (Spectronic Instruments). A 450 W xenon arc lamp was used as the excitation source, and single-grating monochromators served as the wavelength selection devices. The excitation and emission spectral band-pass was typically 1 nm. All emission and excitation spectra were background corrected by using appropriate blanks. Time-resolved fluorescence measurements were carried out by using an IBH model 5000W SAFE time-correlated single photon counting fluorescence lifetime instrument with a N_2-filled flash lamp as our excitation source. The lamp repetition rate was 40 kHz. The excitation wavelength was 337 nm. Single grating monochromators were used to select the desired emission wavelength. The emission spectral band-pass was ≤16 nm. All time-resolved intensity decay profiles were recorded under magic angle polarization conditions. The typical time resolution for an experiment was 0.47 ns/channel, and we used 1024 total channels in the multichannel analyzer (MCA). To avoid pulse pileup, the count rate at the reference and emission detectors was always less than 2% of the flash lamp repetition rate. Data were acquired until there were at least 10^4 counts in the peak MCA channel. The instrument response and the monomer and excimer intensity decay data were always acquired simultaneously.

Two high-pressure spectroscopy systems were used in these experiments. The basic system consists of a microprocessor-controlled syringe pump (Isco model 260-D) that is purged and charged with CO_2 or a binary mixture of CO_2 with 1 mol % MeOH, stainless steel tubing and plumbing, a high-pressure optical cell with fused silica optical windows, and a stainless steel body.[27] Throughout an experiment, the system pressure is regulated by the Isco pump to ±2 psia and monitored by using a calibrated Heise gauge. The cell temperature was maintained at 35 ± 0.1 °C by using four 100 W cartridge heaters (model CIR-1031) that are located within the high-pressure cell's body, a thermocouple probe (model RID-860), and microprocessor-based temperature controller (CN 76000 series) (all from Omega Engineering, Inc.).

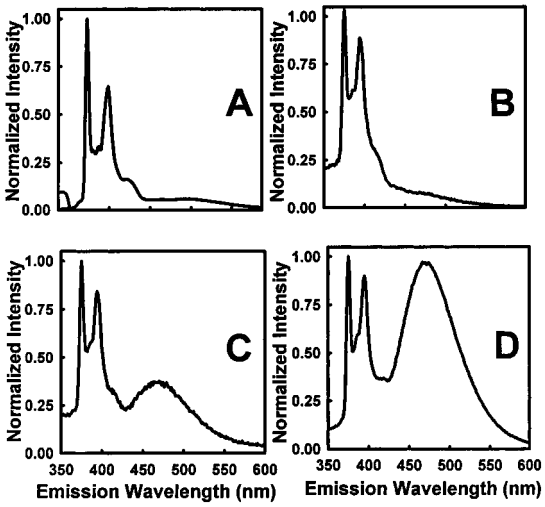

Figure 2. Normalized steady-state emission spectra of Py-PDMS-Py: (panel A) liquid toluene; (panels B, C, and D) scCO_2 at reduced densities of 1.1, 1.6, and 1.8, respectively.

Extended pressure range experiments were performed by using a model HPSC-3K high-pressure spectroscopy system (Spectronic Instruments). The HPSC-3K is a commercially available system that can be operated up to 3 kbar. The system includes an analogue pressure gauge, a digital temperature gauge, a high-pressure hand pump, a high-pressure optical cell, and all the high-pressure plumbing. The cell temperature was maintained at 35 ± 0.1 °C by using a circulating water bath.

Statistics. All experiments were performed at least three times on freshly prepared samples. Results are reported as the average of the individual measurements ±1 standard deviation.

Results and Discussion

Steady-State Fluorescence Studies. Figure 2 presents typical steady-state emission spectra for Py-PDMS-Py dissolved in either liquid toluene or scCO_2. Figure 2A shows the spectrum recorded in liquid toluene at 25 °C. Parts B, C, and D of Figure 2 show spectra recorded in scCO_2 at reduced densities ($\rho_r = \rho_{experiment}/\rho_{critical}$) of 1.1, 1.6, and 1.8, respectively. Emission from the monomer is observed between 370 and 430 nm in all samples. The excimer emission clearly grows in for the Py-PDMS-Py samples in the 440−550 nm region as the CO_2 density is increased. No excimer emission is evident for 1-ethylpyrene, the model monomer, at these same fluorophore concentrations and conditions (spectra not shown).

One must carefully distinguish between classic excimers that form in and exist only in the excited state and related species that appear like an excimer but form from preassociated inter- or intramolecular pyrene species prior to optical excitation.[28,29] Fortunately, one can discriminate between these so-called static dimers and true dynamic excimers by recording the electronic absorbance spectra[28] and/or the emission wavelength-dependent excitation scans.[29] If our Py-PDMS-Py system is described by a purely intramolecular excimer, the normalized emission wavelength-dependent excitation scans will be *independent* of emission wavelength.[29] If these excitation spectra are shifted relative to one another, this is an indication of inter- and/or intramo-

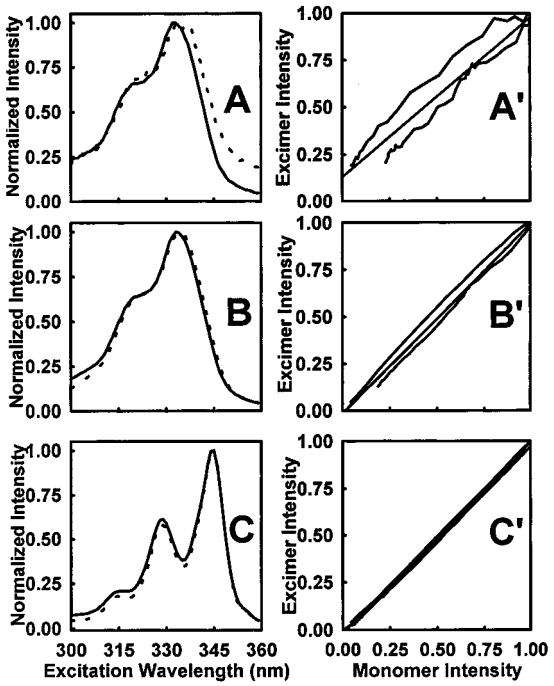

Figure 3. Normalized emission wavelength-dependent excitation spectra and correlation plots for Py-PDMS-Py dissolved in $scCO_2$ or liquid toluene. Monomer (—) and excimer (- - -) scans. (panels A and B) $scCO_2$ at reduced densities of 1.1 and 1.8, respectively. (panel C) Liquid toluene. (panels A′, B′, and C′) Intensity−intensity correlation plots corresponding to panels A, B, and C, respectively.

lecular interactions between the pyrene residues in the ground state.

Figure 3 presents three pairs of normalized emission wavelength-dependent excitation spectra for Py-PDMS-Py dissolved in $scCO_2$ at reduced densities of 1.1 (Figure 3A) and 1.8 (Figure 3B) and in liquid toluene (Figure 3C). The corresponding correlation plots[29] (Figure 3A′,B′,C′) are also presented. The monomer (—) and excimer (- - -) spectra are acquired by adjusting the emission wavelength to that region of the spectrum where each species predominates, 378 and 480 nm, respectively, and recording the appropriate excitation spectra. The results in Figure 3 show that the Py-PDMS-Py ground state in liquid toluene is homogeneous. In fact, previous work from our laboratory argued that the Py-PDMS-Py excimer formation process in liquid toluene followed Scheme 1.[16] The results in Figure 3 argue that (1) the Py-PDMS-Py ground state is not homogeneous in $scCO_2$, (2) Scheme 1 cannot describe the Py-PDMS-Py excimer formation process in $scCO_2$, and (3) the extent of ground-state heterogeneity is greater at lower CO_2 densities and decreases as the CO_2 density increases.

Figure 4 summarizes the effects of CO_2 density on the Py-PDMS-Py excimer-to-monomer intensity ratio (E/M). Several aspects of these data merit further discussion. First, the Py-PDMS-Py E/M changes 15-fold between a reduced density of 0.7 and 2.3. Second, even though the CO_2 viscosity is much less at lower densities[30] and one might expect to see greater excimer emission in the low-density regime, we observe much *less* excimer emission at lower CO_2 densities. Third, although the CO_2 viscosity is increasing with increasing density, the E/M increases systematically as we increase the reduced density from 1.1 to 1.8. Finally, above a reduced density of ~1.8, the E/M appears to roll over

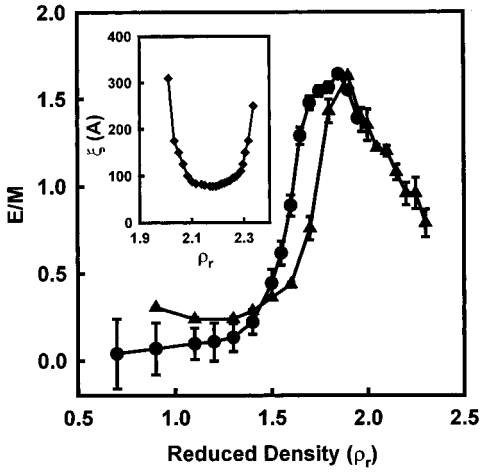

Figure 4. Effects of CO_2 density on the Py-PDMS-Py excimer-to-monomer ratio (E/M). Results using the basic high-pressure optical cell (●) and the extended range cell (▲) are shown. (inset) Effects of CO_2 density on the PDMS chain ($M_w = 47\,700$) correlation length, ξ (from ref 15).

and decrease as we increase the CO_2 density. We discuss these observations in more detail below.

Time-Resolved Fluorescence Studies. Initially we recorded the time-resolved intensity decay traces for dilute 1-ethylpyrene dissolved in $scCO_2$ between a reduced density of 1.40 and 1.95. In all cases, the 1-ethylpyrene intensity decay traces were well described by a single fluorescence lifetime ($\chi^2 \leq 1.12$). The recovered k_M values are collected in Table 1.

Our steady-state fluorescence results (Figures 2−4) suggest that the Py-PDMS-Py behavior is $scCO_2$ is a strong function of the CO_2 density, and it is much different in caparison to Py-PDMS-Py dissolved in liquid toluene. To explore the origin of this behavior, we recorded the time-resolved intensity decay traces at the Py-PDMS-Py "monomer" and "excimer" emission maxima as a function CO_2 density. A typical data set, fits, residuals, and autocorrelation functions for Py-PDMS-Py dissolved in $scCO_2$ at a reduced density of 1.60 is shown in Figure 5. The top panel shows the raw normalized time-resolved intensity decay data for the monomer (●, $\lambda_{em} = 378$ nm) and excimer (○, $\lambda_{em} = 480$ nm), the flash lamp instrument response profile (▲), and the fits between the experimental data and Scheme 2 (—). The central panels present the residues between the fit and the monomer and excimer experimental data, respectively. The lower panels present the corresponding autocorrelation functions for the monomer and excimer decay traces.

Simultaneous global analysis[26] of the monomer and excimer decay data (at a given reduced density) in concert with the independent k_M data from the 1-ethylpyrene experiments (vide supra) were used to model the Py-PDMS-Py intensity decay data. We initially tried to model the Py-PDMS-Py/$scCO_2$ intensity decay data by using Scheme 1. Unfortunately, the fits were always poor ($\chi^2_{global} \geq 17$), the residuals were large and nonrandom, and the autocorrelation functions were unacceptable (results not shown). On the basis of our steady-state data (Figure 3), we then tried to model the Py-PDMS-Py/$scCO_2$ intensity decay data by using Scheme 2. Fits to Scheme 2 were always good (cf. Figure 5), the χ^2_{global} was ≤1.2, the Durbin−Watson parameter[31] was ≥1.9, and the residuals and autocorrelation functions were randomly distributed about zero. On the basis of

Table 1. Recovered Rates Describing the Py-PDMS-Py Photophysics in $scCO_2$[a]

ρ_r	k_{cycl} (10^8 s^{-1})	k_{unfol} (10^7 s^{-1})	k_M (10^7 s^{-1})[b]	k_E (10^7 s^{-1})	α	$K^* = k_1/k_{-1}$
1.40	2.44 ± 0.21	1.83 ± 0.52	4.75 ± 0.05	2.90 ± 0.16	0.14 ± 0.03	13.3 ± 2.11
1.50	2.59 ± 0.25	1.97 ± 0.11	5.08 ± 0.10	3.72 ± 0.04	0.42 ± 0.05	13.1 ± 1.46
1.55	2.73 ± 0.25	2.62 ± 0.09	5.22 ± 0.07	3.73 ± 0.01	0.57 ± 0.03	10.4 ± 0.75
1.60	2.19 ± 0.12	2.77 ± 0.04	5.36 ± 0.04	3.80 ± 0.01	0.62 ± 0.02	7.91 ± 0.21
1.65	2.05 ± 0.14	2.99 ± 0.25	5.47 ± 0.02	3.82 ± 0.01	0.72 ± 0.01	6.86 ± 0.25
1.70	1.92 ± 0.13	3.09 ± 0.14	5.55 ± 0.01	3.90 ± 0.01	0.72 ± 0.01	6.21 ± 0.30
1.75	1.73 ± 0.12	2.71 ± 0.09	5.72 ± 0.05	4.00 ± 0.01	0.75 ± 0.02	6.38 ± 0.24
1.80	1.51 ± 0.10	2.23 ± 0.05	5.76 ± 0.04	4.03 ± 0.07	0.74 ± 0.01	6.77 ± 0.18
1.85	1.44 ± 0.04	2.22 ± 0.04	5.78 ± 0.04	4.02 ± 0.01	0.79 ± 0.01	6.49 ± 0.12
1.90	1.26 ± 0.03	2.22 ± 0.02	5.81 ± 0.02	3.96 ± 0.02	0.83 ± 0.01	5.68 ± 0.16
1.95	1.13 ±0.02	2.16 ± 0.09	5.79 ± 0.08	3.78 ± 0.02	0.85 ± 0.01	5.23 ± 0.22

[a] See Scheme 2 for a description of all terms. [b] From separate measurements of 1-ethylpyrene.

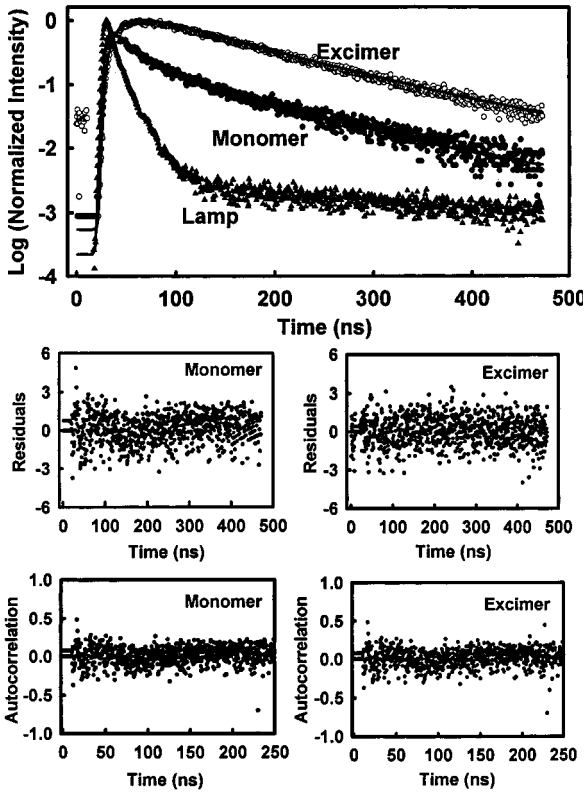

Figure 5. Typical time-correlated single photon counting data, instrument response function, fits, residuals, and autocorrelation functions for Py-PDMS-Py dissolved in $scCO_2$ at a reduced density of 1.60. Monomer monitored at $\lambda_{em} = 378$ nm (●). Excimer monitored at $\lambda_{em} = 480$ nm (○). The solid curves passing through the data (upper panel) are the best fit to Scheme 2.

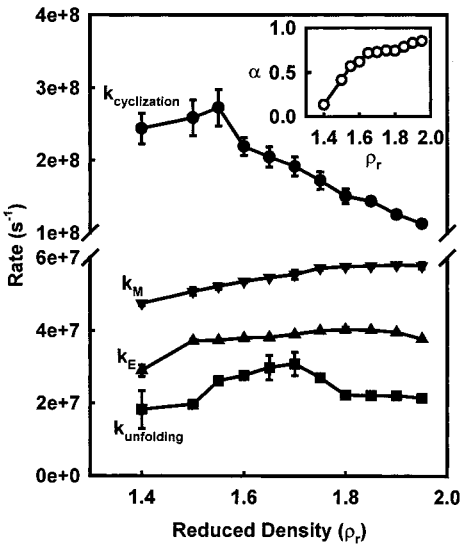

Figure 6. Effects of CO_2 density on the Py-PDMS-Py unimolecular cyclization ($k_{cyclization}$), unfolding ($k_{unfolding}$), excimer decay (k_E), and monomer decay (k_M) rates. (inset) Density dependence of α.

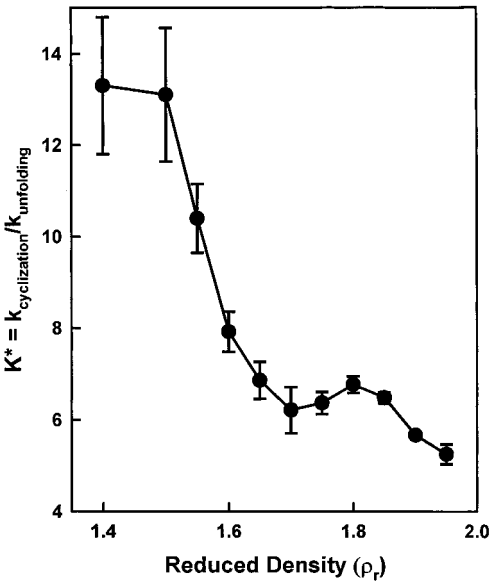

Figure 7. Effects of CO_2 density on the apparent Py-PDMS-Py excited-state equilibrium constant (K^*).

all these assessments of fit quality, we opted to use Scheme 2 to model the Py-PDMS-Py excimer formation process in $scCO_2$.

Table 1 compiles the recovered kinetic terms (see Scheme 2) that describe the behavior of Py-PDMS-Py dissolved in $scCO_2$ between a reduced density of 1.40 and 1.95. (Note: we are currently unable to perform time-resolved experiments above a reduced density of 1.95 because we cannot fit the extended pressure cell body within our IBH 5000 W SAFE instrument.) For ease of visualization Table 1 data are presented graphically in Figures 6 and 7.

Figure 6 summarizes the effects of CO_2 density on $k_{cyclization}$, $k_{unfolding}$, k_M, k_E, and α. Several aspects of these results merit further discussion. First, the Py-PDMS-Py monomer decay rate (k_M) is always greater, by about 2-fold, in comparison to the excimer (k_E) decay rate. Second, k_M and k_E increase slightly (~10−25%) as the CO_2 density increases. Third, given our measurement imprecision, the unfolding rate ($k_{unfolding}$) is essentially independent of CO_2 density. Thus, changes in the CO_2 density appear to neither assist nor inhibit the Py-PDMS-Py tail segments from unfolding following the excimer formation event. Fourth, the rate with which

the Py-PDMS-Py tails can cyclize ($k_{cyclization}$) decreases by ~3-fold as the CO_2 density increases. This indicates that the actual rate with which the Py-PDMS-Py tails in the unconstrained species can cyclize is greater when the CO_2 density is lower. This result is consistent with the density dependence of CO_2 viscosity.[30] Finally, the percentage of ground-state Py-PDMS-Py molecules that are in a form that is able to cyclize (α) increases from about 14% at a reduced density of 1.40 up to 85% at a reduced density of 1.95. Overall, the data presented in Figure 6 show that the unique behavior of Py-PDMS-Py when it is dissolved in $scCO_2$ arises from $k_{cyclization}$ and α with α being the key factor.

Several authors have used the apparent excited-state equilibrium constant ($K^* = k_{cyclization}/k_{unfolding}$) as a tool to assess the conformation of tail-labeled polymers dissolved in liquids.[21] Figure 7 illustrates the effects of CO_2 density on the Py-PDMS-Py K^*. These results show that K^* decreases as the CO_2 density increases, suggesting that the mean-free distance between those polymer tail segments in the ground state that are *able* to cyclize and form an excimer is actually less at lower CO_2 densities.

Origin of the Density-Dependent α Term. By themselves our $k_{cyclization}$ (Figure 6) and K^* (Figure 7) data argue that there should be more excimer emission at the lower CO_2 densities; however, the α term dominates and one actually observes less excimer at the lower CO_2 densities. Given this, we focus now on identifying the causes behind the density-dependent α term.

Farinha et al.[21g] have investigated the behavior of polystyrene (PS, M_n = 10 600) dissolved in liquid cyclohexane that was end-labeled with 4-(1-pyrenyl) butanoamide. This species (Py-PS-Py), like our Py-PDMS-Py (Figure 1), possesses peptide bonds near the chain termini. Farinha et al. found that their fluorescence spectra were consistent with a heterogeneous ground state, and they argued that the Py-PS-Py underwent *intrachain* hydrogen bonding wherein the amide hydrogen near one chain termini hydrogen-bonded to the carbonyl residue at the opposing termini of the same PS chain. This intramolecular hydrogen bonding resulted in two forms of Py-PS-Py (i.e., non-hydrogen-bonded and intramolecularly hydrogen-bonded) that exist simultaneously in the ground state prior to photoexcitation. Our Py-PDMS-Py data are consistent with the existence of non-hydrogen-bonded and intramolecularly hydrogen-bonded forms of Py-PDMS-Py in $scCO_2$. At low CO_2 densities the intramolecularly hydrogen-bonded form appears to dominate, but this species *cannot* cyclize to form a normal excimer during the Py residue's excited-state lifetime. We have ruled out intermolecular Py-PDMS-Py processes because the E/M at a given CO_2 density did not change significantly when we changed the Py-PDMS-Py concentration more than 20-fold (results not shown). Our proposed scenario is also consistent with results from Tsugane et al.,[32] who studied the density dependence of benzoic acid intermolecular dimerization and hydrogen bonding in $scCO_2$. These authors found that there was a greater degree of intermolecular hydrogen bonding and dimerization at lower CO_2 densities.

In an effort to confirm our suspicion regarding the origin of the density-dependent α results, we investigated the behavior of Py-PDMS-Py dissolved in a binary supercritical fluid composed of CO_2 and 1 mol % MeOH.

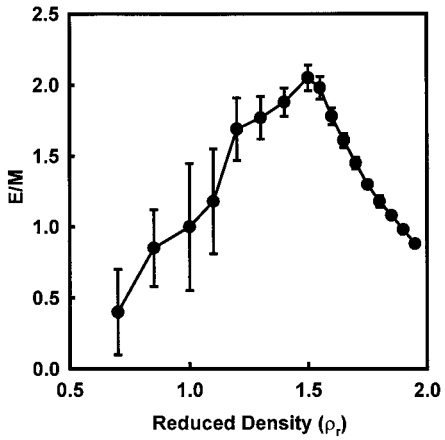

Figure 8. Effects of density on the Py-PDMS-Py excimer-to-monomer ratio (E/M) in a binary mixture that contains CO_2 and 1 mol % MeOH.

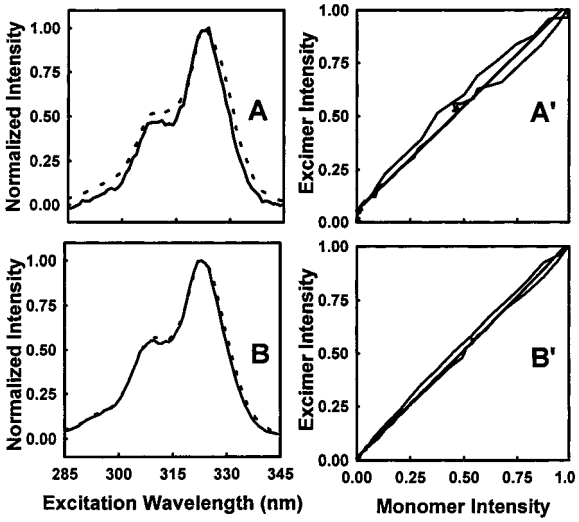

Figure 9. Normalized emission wavelength-dependent excitation spectra and correlation plots for Py-PDMS-Py dissolved in a binary mixture that contains CO_2 and 1 mol % MeOH. Monomer (—) and excimer (- - -) scans. (panels A and B) $scCO_2$ at reduced densities of 1.1 and 1.8, respectively. (panels A′ and B′) Intensity−intensity correlation plots corresponding to panels A and B, respectively.

Our idea was that the MeOH would disrupt intramolecular hydrogen bonding, free up the Py-PDMS-Py tails, and produce a concomitant increase in excimer formation. Figure 8 summarizes the results of this experiment. In comparison to the results in $scCO_2$ (Figure 4), one sees significantly more excimer emission in the low-density region when the MeOH is added to the CO_2. This result is consistent with MeOH disrupting some of the intermolecular hydrogen bonding.

If the MeOH disrupts the constrained (i.e., hydrogen bonded) form(s) of Py-PDMS-Py in the ground state, one would also anticipate seeing less ground-state heterogeneity in the Py-PDMS-Py system in the presence of the MeOH cosolvent. Figure 9 presents a set of emission wavelength-dependent excitation scans for Py-PDMS-Py when it is dissolved in a binary supercritical fluid composed of CO_2 and 1 mol % MeOH at reduced densities of 1.1 (Figure 9A) and 1.8 (Figure 9B). The corresponding intensity−intensity correlation plots are shown in parts A′ and B′ of Figure 9, respectively. In comparison to Py-PDMS-Py spectra in $scCO_2$ (Figure 3), one can see that the Py-PDMS-Py ground state in the

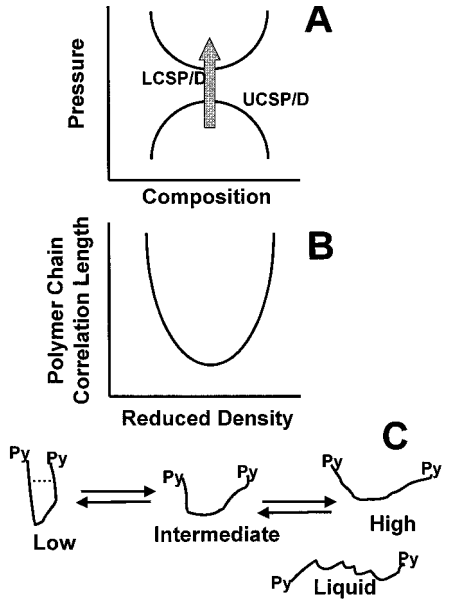

Figure 10. Summary of the Py-PDMS-Py behavior in $scCO_2$. (panel A) Pressure/density-dependent upper (UCSP/D) and lower critical solution pressures/densities (LCSP/D). (panel B) Density-dependent PDMS chain correlation length. (panel C) Density-dependent intermolecular hydrogen-bonding and changes in the tail segment mean-free distances.

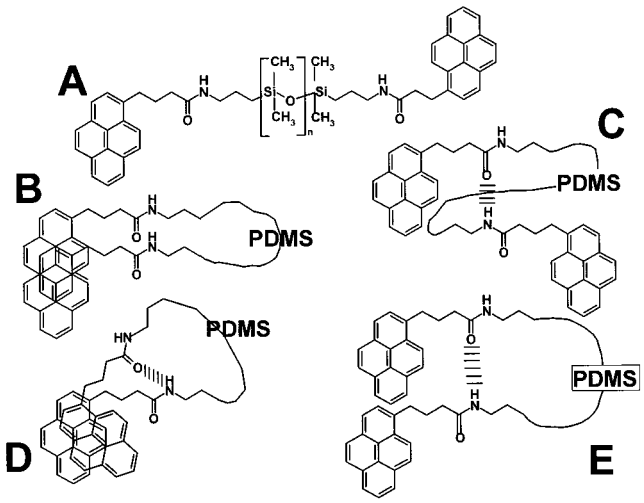

Figure 11. Hypothetical structures of the Py-PDMS-Py ground-state species induced by intramolecular hydrogen bonding.

presence of the small amount of MeOH cosolvent is clearly more homogeneous.

The E/M Rollover at High CO_2 Densities. In the critical region the CO_2 viscosity is a strong function of pressure,[30] so changes in fluid viscosity can be used to explain a portion of the E/M density dependence. However, above a reduced density of ~1.5, the CO_2 viscosity does not change appreciably with increasing density and viscosity alone cannot be used to explain the 2-fold decrease in the Py-PDMS-Py E/M between a reduced density of 1.9 and 2.3 (Figure 4). It is also difficult to use an intramolecular hydrogen-bonding argument to explain the results at high density because the Py-PDMS-Py ground state appears to be nearly homogeneous above a reduced density of ~2.0 (Figure 3). Thus, there must be one or more additional reason(s) for the drop in E/M at higher CO_2 densities that is not associated with the heterogeneity of the Py-PDMS-Py ground state or the CO_2 viscosity per se. Two possibilities come to mind as we increase the CO_2 density: (1) an increase in the mean-free distance between the Py-PDMS-Py tails and/or (2) the PDMS chains themselves becoming less dynamic.

Our previous work on Py-PDMS-Py dissolved in liquid toluene (a good solvent for PDMS) exhibited a K^* of 0.52 ± 0.10.[16] Our lowest K^* value for Py-PDMS-Py dissolved in $scCO_2$ is >5 (Figure 7). These results suggest that the PDMS chains in Py-PDMS-Py are *never* fully extended at any of the CO_2 densities investigated here.

In an elegant series of experiments Melnichenko et al.[15] reported the effects of CO_2 density on the correlation length, ξ, of 47 700 MW PDMS at 32 °C (Figure 4 inset, ◆). These results were explained in terms of an upper critical solution pressure (UCSP) where the system exhibited pressure-induced phase demixing. With an increase in pressure, ξ goes through a minimum after which the lower critical solution pressure (LCSP) is approached. Our Py-PDMS-Py E/M data appear to follow a similar trend given the anticipated shift in our profile toward lower densities because our PDMS chains are shorter in comparison to those studied by Melnichenko et al.[15] Thus, our Py-PDMS-Py results also appear to be consistent with the intrachain PDMS dynamics decreasing with an increase in CO_2 density in line with the changes in the PDMS ξ.

Conclusions

The behavior of polymers dissolved in $scCO_2$ can be quite different than their behavior in normal liquids (Figure 10). The Py-PDMS-Py (Figure 1) case is illustrative. In a good solvent like toluene, the Py-PDMS-Py excimer formation can be modeled by Scheme 1.[16] When Py-PDMS-Py is dissolved in $scCO_2$, there appear to be at least two forms of Py-PDMS-Py in the ground state: constrained and unconstrained. The constrained species arises from intramolecular hydrogen bonding between the peptide segments that are located near the Py-PDMS-Py terminal region. The constrained species does not allow normal excimers to form, and it is the dominant species at lower CO_2 densities. As one increases the CO_2 density, the intramolecular hydrogen bonding is disrupted and more excimer is formed. This result is consistent with related work on the intermolecular dimerization of benzoic acid in $scCO_2$.[32] The mean-free distance between the Py-PDMS-Py termini also appears to be density dependent. At low CO_2 densities, the Py residues on the unconstrained Py-PDMS-Py species are closer together on average than they are at higher CO_2 densities. This result is consistent with continuous space Monte Carlo simulations on the effects of solvent density on the mean-square end-to-end distances of a single chain monomer with 20 Lennard-Jones segments dissolved in a monomeric solvent.[14b] Our data also suggest that the PDMS chain in Py-PDMS-Py is never completely extended (unlike its behavior in toluene) at any CO_2 density studied. As the CO_2 reduced density is increased beyond ~1.9, the Py-PDMS-Py excimer-to-monomer intensity ratio begins to decrease significantly. At these high CO_2 densities the intramolecular hydrogen bonding is nearly all disrupted so we suggest that the observed decrease in the excimer emission arises from our approach to the lower critical solution pressure/density and the concomitant increase in the PDMS chain correlation length.[15]

We are attempting to determine the actual structure of the ground-state Py-PDMS-Py species (Figure 11) by

recording the decay associated spectra[33] and exploring the possibility of multiple excimer-like species.[34] Additional experiments with a Py-PDMS-Py species that cannot form intramolecular hydrogen bonds are also planned.

Acknowledgment. This work was generously supported by the Department of Energy (DEFG0290ER-14143). We also thank Gary Sagerman and Gary Nottingham of the College of Arts & Sciences Machine Shop at the University at Buffalo, The State University of New York, for their help.

References and Notes

(1) Sperling, L. H. *Introduction to Physical Polymer Science*, 2nd ed.; John Wiley & Sons: New York, 1992.
(2) Stevens, M. P. *Polymer Chemistry*: *An Introduction*, 2nd ed.; Oxford University Press: New York, 1990.
(3) Kovarskii, A. L., Ed. *High-Pressure Chemistry and Physics of Polymers*; CRC Press: Boca Raton, FL, 1994.
(4) (a) Via, J.; Taylor, L. T. *CHEMTECH* **1993**, *24*, 38. (b) Noble, D. *Anal. Chem*. **1993**, *65*, 693A.
(5) Johnston, K. P., Penninger, J. M. L., Eds. *Supercritical Fluid Science and Technology*; ACS Symposium Series Vol. 406; American Chemical Society: Washington, DC, 1989.
(6) Bruno, T. J.; Ely, J. F. *Supercritical Fluid Technology-Reviews in Modern Theory and Applications*; CRC Press: Boca Raton, FL, 1991.
(7) Bright, F. V., McNally, M. E. P., Eds. *Supercritical Fluid Technology-Theoretical and Applied Approaches in Analytical Chemistry*; ACS Symposium Series Vol. 488; American Chemical Society: Washington, DC, 1992.
(8) Kiran, E., Brennecke, J. F., Eds. *Supercritical Fluid Engineering Science-Fundamentals and Applications*; ACS Symposium Series Vol. 514; American Chemical Society: Washington, DC, 1993.
(9) McHugh, M. A.; Krukonis, V. J. *Supercritical Fluids Extraction*: *Priniciples and Practice*, 2nd ed.; Butterworth-Heinemann: Boston, 1994.
(10) Kiran, E., Sengers, J. M. H. L., Eds. *Supercritical Fluids*. *Fundamentals for Applications*; Kluwer Academic: Dordrecht, 1994.
(11) Noyori, R., Ed. *Chem. Rev*. **1999**, *99*, 353.
(12) Jessop, P. G., Leitner, W., Eds. *Chemical Synthesis Using Supercritical Fluids*; Wiley-VCH: New York, 1999.
(13) (a) DeSimone, J. M.; Guan, Z.; Elsbernd, C. S. *Science* **1992**, *257*, 945. (b) DeSimone, J. M.; Maury, E. E.; Menceloglu, Y. Z.; McClain, J. B.; Romack, T. J.; Combes, J. R. *Science* **1994**, *265*, 356. (c) Kendall, J. L.; Canelas, D. A.; Young, J. L.; DeSimone, J. M. *Chem. Rev*. **1999**, *99*, 543.
(14) There have been several theoretical efforts on this issue: (a) Gromov, D. G.; de Pablo, J. J.; Luna-Barcenas, G.; Sanchez, I. C.; Johnston, K. P. *J. Chem. Phys*. **1998**, *108*, 4647. (b) Luna-Barcenas, G.; Meredith, J. C.; Sanchez, I. C.; Johnston, K. P.; Gromov, D. G.; de Pablo, J. J. *J. Chem. Phys*. **1997**, *107*, 10782. (c) Luna-Barcenas, G.; Gromov, D. G.; Meredith, J. C.; Sanchez, I. C.; de Pablo, J. J.; Johnston, K. P. *Chem. Phys. Lett*. **1997**, *278*, 302.
(15) Melnichenko, Y. B.; Kiran, E.; Wignall, G. D.; Heath, K. D.; Salaniwal, S.; Cochran, H. D.; Stamm, M. *Macromolecules* **1999**, *32*, 5344.
(16) Kane, M. A.; Baker, G. A.; Pandey, S.; Maziarz, E. P. III; Hoth, D. C.; Bright, F. V. *J. Phys. Chem. B* **2000**, *104*, 8585.
(17) Cooper, A. I.; DeSimone, J. M. *Cur. Opin. Solid State Mater. Sci*. **1996**, *1*, 761 and references therein.
(18) Kendall, J. L.; Canelas, D. A.; Young, J. L.; DeSimone, J. M. *Chem. Rev*. **1999**, *99*, 543 and references therein.
(19) Cuniberti, C.; Perico, A. *Eur. Polym. J*. **1977**, *13*, 369.
(20) *Photophysical and Photochemical Tools in Polymer Science*; Winnik, M. A., Ed.; D. Reidel Co.: Dordrecht, 1986.
(21) (a) Redpath, A. E. C.; Winnik, M. A. *J. Am. Chem. Soc*. **1982**, *104*, 5604. (b) Winnik, M. A. *Acc. Chem. Res*. **1985**, *18*, 73. (c) Svirskaya, P.; Danhelka, J.; Redpath, A. E. C.; Winnik, M. A. *Polymer* **1983**, *24*, 319. (d) Martinho, J. M. G.; Reis e Sousa, A. T.; Winnik, M. A. *Macromolecules* **1993**, *26*, 4484. (e) Martinho, J. M. G.; Castanheira, E. M. S.; Reis e Sousa, A. T.; Saghbini, S.; André, J. C.; Winnik, M. A. *Macromolecules* **1995**, *28*, 1167. (f) Reis e Sousa, A. T.; Castanheira, E. M. S.; Martinho, J. M. G.; Saghbini, S.; Baros, F.; André, J. C.; Winnik, M. A. *Chem. Phys. Lett*. **1993**, *213*, 333. (g) Farinha, P. S.; Martinho, J. M. G.; Xu, H.; Winnik, M. A.; Quirk, R. P. *J. Polym. Sci., Polym. Phys. B* **1994**, *32*, 1635.
(22) Birks, J. B. *Photophysics of Aromatic Molecules*; Wiley-Interscience: London, 1970; Chapter 7.
(23) Klöpffer, W. In *Organic Molecular Photophysics*; Birks, J. B., Ed.; John Wiley & Sons: New York, 1973; Vol. 1, Chapter 7.
(24) The additional assumption is made that the molar absorptivity for the unconstrained and constrained forms of Py-PDMS-Py are equivalent.
(25) Andriessen, R.; Boens, N.; Ameloot, M.; De Schryver, F. C. *J. Phys. Chem*. **1991**, *95*, 2047.
(26) Beechem, J. M.; Gratton, E.; Ameloot, M.; Knutson, J. R.; Brand, L. In *Topics in Fluorescence Spectroscopy*; Lakowicz, J. R., Ed.; Plenum Press: New York, 1991; Vol. 2, Chapter 5.
(27) Betts, T. A.; Bright, F. V. *Appl. Spectrosc*. **1990**, *44*, 1196.
(28) Winnik, F. M. *Chem. Rev*. **1993**, *93*, 587.
(29) Zagrobelny, J.; Betts, T. A.; Bright, F. V. *J. Am. Chem. Soc*. **1992**, *114*, 5249.
(30) Reid, R. C.; Prausnitz, J. M.; Poling, B. E. *The Properties of Gases and Liquids*, 4th ed.; McGraw-Hill: New York, 1987; Chapter 9.
(31) Nakasuji, K.; Akiyama, S.; Nakagawa, M. *Bull. Chem. Soc. Jpn*. **1972**, *45*, 5, 875.
(32) Tsugane, H.; Yagi, Y.; Inomata, H. *J. Chem. Eng. Jpn*. **1992**, *25*, 351.
(33) (a) Badea, M. G.; Brand, L. *Methods Enzymol*. **1979**, *61*, 378. (b) Knutson, J. R.; Walbridge, D. G.; Brand, L. *Biochemistry* **1982**, *21*, 4671. (c) Green, S.; Knutson, J. R.; Hensley, P. *Biochemistry* **1990**, *29*, 9159. (d) Beechem, J. M.; Knutson, J. R.; Ross, J. B. A.; Turner, B. W.; Brand, L. *Biochemistry* **1983**, *22*, 6054. (e) Knutson, J. R.; Beechem, J. M.; Brand, L. *Chem. Phys. Lett*. **1983**, *102*, 501. (f) Beechem, J. M.; Ameloot, M.; Brand, L. *Chem. Phys. Lett*. **1985**, *120*, 466.
(34) (a) Kawashima, T.; Otsubo, T.; Sakata, Y.; Misumi, S. *Tetrahedron Lett*. **1979**, 5115. (b) Staab, H. A.; Riegler, N.; Diederich, F.; Krieger, C.; Schweitzer, D. *Chem. Ber*. **1984**, *117*, 246. (c) Yamazaki, T.; Tamai, N.; Yamazaki, I. *Chem. Phys. Lett*. **1986**, *124*, 326. (d) Taniguchi, Y.; Mitsuya, M.; Tamai, N.; Yamazaki, I.; Masuhara, H. *Chem Phys. Lett*. **1986**, *132*, 516. (e) Yamazaki, I.; Tamai, N.; Yamazaki, T. *J. Phys. Chem*. **1987**, *91*, 3572. (f) Yamazaki, I.; Winnik, F. M.; Winnik, M. A.; Tazuke, S. *J. Phys. Chem*. **1987**, *91*, 4213. (g) Kitamura, T.; Takahashi, Y.; Yamanaka, T.; Uchida, K. *J. Lumin*. **1991**, *48 & 49*, 373. (h) Winnik, F. M.; Tamai, N.; Yonezawa, J.; Nishimura, Y.; Yamazaki, I. *J. Phys. Chem*. **1992**, *96*, 1967. (i) Tsujii, Y.; Itoh, T.; Fukuda, T.; Miyamoto, T.; Ito, S.; Yamamoto, M. *Langmuir* **1992**, *8*, 936. (j) Declercq, D.; Delbeke, P.; De Schryver, F. C.; Van Meervelt, L.; Miller, R. D. *J. Am. Chem. Soc*. **1993**, *115*, 5702. (k) Zilberstein, J.; Bromberg, A.; Berkovic, G. *J. Photochem. Photobiol. A.*: *Chem*. **1994**, *77*, 69. (l) Dutta, A. K.; Misra, T. N.; Pal, A. J. *Langmuir* **1996**, *12*, 459.

MA010837U